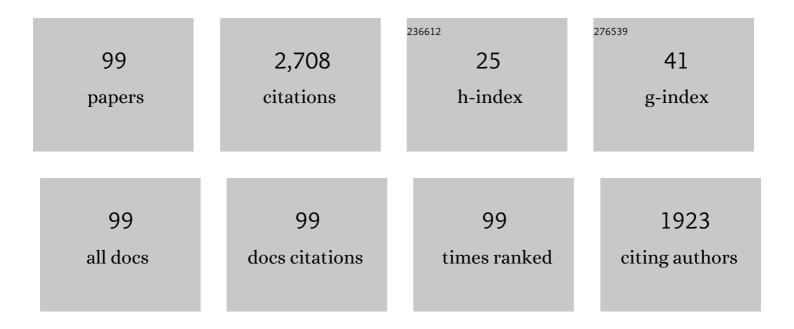
David Alonso-Caneiro

List of Publications by Year in descending order

Source: https://exaly.com/author-pdf/6106387/publications.pdf Version: 2024-02-01



#	Article	IF	CITATIONS
1	Choroidal Thickness in Myopic and Nonmyopic Children Assessed With Enhanced Depth Imaging Optical Coherence Tomography. , 2013, 54, 7578.		160
2	Choroidal Thickness in Childhood. , 2013, 54, 3586.		138
3	Longitudinal Changes in Choroidal Thickness and Eye Growth in Childhood. , 2015, 56, 3103.		126
4	Automatic segmentation of choroidal thickness in optical coherence tomography. Biomedical Optics Express, 2013, 4, 2795.	1.5	107
5	Choroidal changes in human myopia: insights from optical coherence tomography imaging. Australasian journal of optometry, The, 2019, 102, 270-285.	0.6	99
6	Assessment of corneal dynamics with high-speed swept source Optical Coherence Tomography combined with an air puff system. Optics Express, 2011, 19, 14188.	1.7	92
7	Automatic segmentation of OCT retinal boundaries using recurrent neural networks and graph search. Biomedical Optics Express, 2018, 9, 5759.	1.5	92
8	Effect of patch size and network architecture on a convolutional neural network approach for automatic segmentation of OCT retinal layers. Biomedical Optics Express, 2018, 9, 3049.	1.5	91
9	Regional Changes in Choroidal Thickness Associated With Accommodation. , 2015, 56, 6414.		86
10	Automatic choroidal segmentation in OCT images using supervised deep learning methods. Scientific Reports, 2019, 9, 13298.	1.6	82
11	Hypoxic Corneal Changes following Eight Hours of Scleral Contact Lens Wear. Optometry and Vision Science, 2016, 93, 293-299.	0.6	72
12	Speckle reduction in optical coherence tomography imaging by affine-motion image registration. Journal of Biomedical Optics, 2011, 16, 116027.	1.4	64
13	Corneal changes following short-term miniscleral contact lens wear. Contact Lens and Anterior Eye, 2014, 37, 461-468.	0.8	59
14	Anterior eye tissue morphology: Scleral and conjunctival thickness in children and young adults. Scientific Reports, 2016, 6, 33796.	1.6	59
15	The temporal dynamics of miniscleral contact lenses: Central corneal clearance and centration. Contact Lens and Anterior Eye, 2018, 41, 162-168.	0.8	57
16	Morphological changes in the conjunctiva, episclera and sclera following short-term miniscleral contact lens wear in rigid lens neophytes. Contact Lens and Anterior Eye, 2016, 39, 53-61.	0.8	56
17	MACULAR RETINAL LAYER THICKNESS IN CHILDHOOD. Retina, 2015, 35, 1223-1233.	1.0	50
18	Wide-field choroidal thickness in myopes and emmetropes. Scientific Reports, 2019, 9, 3474.	1.6	50

#	Article	IF	CITATIONS
19	Predicting Dry Eye Using Noninvasive Techniques of Tear Film Surface Assessment. , 2011, 52, 751.		48
20	Optical coherence tomography and scleral contact lenses: clinical and research applications. Australasian journal of optometry, The, 2019, 102, 224-241.	0.6	40
21	Tissue thickness calculation in ocular optical coherence tomography. Biomedical Optics Express, 2016, 7, 629.	1.5	38
22	Miniscleral lens wear influences corneal curvature and optics. Ophthalmic and Physiological Optics, 2016, 36, 100-111.	1.0	36
23	The time course and nature of corneal oedema during sealed miniscleral contact lens wear. Contact Lens and Anterior Eye, 2019, 42, 49-54.	0.8	35
24	Tear Film Surface Quality With Soft Contact Lenses Using Dynamic-Area High-Speed Videokeratoscopy. Eye and Contact Lens, 2009, 35, 227-231.	0.8	34
25	Longitudinal changes in macular retinal layer thickness in pediatric populations: Myopic vs non-myopic eyes. PLoS ONE, 2017, 12, e0180462.	1.1	34
26	Daily morning light therapy is associated with an increase in choroidal thickness in healthy young adults. Scientific Reports, 2018, 8, 8200.	1.6	34
27	Noninvasive In Vivo Assessment of Soft Contact Lens Type on Tear Film Surface Quality. , 2012, 53, 525.		33
28	Diurnal variation of anterior scleral and conjunctival thickness. Ophthalmic and Physiological Optics, 2016, 36, 279-289.	1.0	33
29	Influence of the time of day on axial length and choroidal thickness changes to hyperopic and myopic defocus in human eyes. Experimental Eye Research, 2019, 182, 125-136.	1.2	31
30	Lateral shearing interferometry, dynamic wavefront sensing, and high-speed videokeratoscopy for noninvasive assessment of tear film surface characteristics: a comparative study. Journal of Biomedical Optics, 2010, 15, 037005.	1.4	29
31	A deep learning method for automatic segmentation of the bony orbit in MRI and CT images. Scientific Reports, 2021, 11, 13693.	1.6	28
32	Peripapillary choroidal thickness in childhood. Experimental Eye Research, 2015, 135, 164-173.	1.2	27
33	Using Optical Coherence Tomography to Assess Corneoscleral Morphology After Soft Contact Lens Wear. Optometry and Vision Science, 2012, 89, 1619-1626.	0.6	26
34	Automatic Detection of Cone Photoreceptors With Fully Convolutional Networks. Translational Vision Science and Technology, 2019, 8, 10.	1.1	26
35	Scleral contact lens thickness profiles: The relationship between average and centre lens thickness. Contact Lens and Anterior Eye, 2019, 42, 55-62.	0.8	25
36	Choroidal Thickness in Young Adults and its Association with Visual Acuity. American Journal of Ophthalmology, 2020, 214, 40-51.	1.7	25

DAVID ALONSO-CANEIRO

#	Article	IF	CITATIONS
37	Diurnal Variation of Retinal Thickness with Spectral Domain OCT. Optometry and Vision Science, 2012, 89, 611-619.	0.6	24
38	Evidence on scleral contact lenses and intraocular pressure. Australasian journal of optometry, The, 2017, 100, 87-88.	0.6	24
39	Assessment of Tear Film Surface Quality Using Dynamic-Area High-Speed Videokeratoscopy. IEEE Transactions on Biomedical Engineering, 2009, 56, 1473-1481.	2.5	23
40	Validation of Optical Low Coherence Reflectometry Retinal and Choroidal Biometry. Optometry and Vision Science, 2011, 88, 855-863.	0.6	23
41	Tear Film Surface Quality With Rigid and Soft Contact Lenses. Eye and Contact Lens, 2012, 38, 171-178.	0.8	23
42	Retinal Boundary Segmentation in Stargardt Disease Optical Coherence Tomography Images Using Automated Deep Learning. Translational Vision Science and Technology, 2020, 9, 12.	1.1	23
43	Diagnosing dry eye with dynamic-area high-speed videokeratoscopy. Journal of Biomedical Optics, 2011, 16, 076012.	1.4	22
44	Anterior scleral thickness changes with accommodation in myopes and emmetropes. Experimental Eye Research, 2018, 177, 96-103.	1.2	22
45	Wideâ€field choroidal thickness and vascularity index in myopes and emmetropes. Ophthalmic and Physiological Optics, 2021, 41, 1308-1319.	1.0	20
46	Estimating Corneal Surface Topography in Videokeratoscopy in the Presence of Strong Signal Interference. IEEE Transactions on Biomedical Engineering, 2008, 55, 2381-2387.	2.5	18
47	The influence of centre thickness on miniscleral lens flexure. Contact Lens and Anterior Eye, 2019, 42, 63-69.	0.8	18
48	Effect of Altered OCT Image Quality on Deep Learning Boundary Segmentation. IEEE Access, 2020, 8, 43537-43553.	2.6	18
49	Deep feature loss to denoise OCT images using deep neural networks. Journal of Biomedical Optics, 2021, 26, .	1.4	17
50	Repeatability of wideâ€field choroidal thickness measurements using enhancedâ€depth imaging optical coherence tomography. Australasian journal of optometry, The, 2019, 102, 327-334.	0.6	14
51	Corneal tissue properties following scleral lens wear using Scheimpflug imaging. Ophthalmic and Physiological Optics, 2020, 40, 595-606.	1.0	13
52	Enhanced Visualization of Subtle Outer Retinal Pathology by En Face Optical Coherence Tomography and Correlation with Multi-Modal Imaging. PLoS ONE, 2016, 11, e0168275.	1.1	12
53	Retinal OFF-Pathway Overstimulation Leads to Greater Accommodation-Induced Choroidal Thinning. , 2021, 62, 5.		12
54	Application of texture analysis in tear film surface assessment based on videokeratoscopy. Journal of Optometry, 2013, 6, 185-193.	0.7	11

#	Article	IF	CITATIONS
55	Impact of image averaging on wideâ€field choroidal thickness measurements using enhancedâ€depth imaging optical coherence tomography. Australasian journal of optometry, The, 2019, 102, 320-326.	0.6	11
56	Glaucoma classification based on scanning laser ophthalmoscopic images using a deep learning ensemble method. PLoS ONE, 2021, 16, e0252339.	1.1	11
57	Induced Refractive Error Changes the Optical Coherence Tomography Angiography Transverse Magnification and Vascular Indices. American Journal of Ophthalmology, 2021, 229, 230-241.	1.7	11
58	Posterior Choroidal Stroma Reduces Accuracy of Automated Segmentation of Outer Choroidal Boundary in Swept Source Optical Coherence Tomography. , 2018, 59, 4404.		10
59	Comparison of Choroidal Thickness Measurements Using Semiautomated and Manual Segmentation Methods. Optometry and Vision Science, 2020, 97, 121-127.	0.6	10
60	Data augmentation for patch-based OCT chorio-retinal segmentation using generative adversarial networks. Neural Computing and Applications, 2021, 33, 7393-7408.	3.2	10
61	Regional Variations in Postlens Tear Layer Thickness During Scleral Lens Wear. Eye and Contact Lens, 2020, 46, 368-374.	0.8	9
62	Macular Thickness Profile and Its Association With Best-Corrected Visual Acuity in Healthy Young Adults. Translational Vision Science and Technology, 2021, 10, 8.	1.1	9
63	Choroidal Thickening During Young Adulthood and Baseline Choroidal Thickness Predicts Refractive Error Change. , 2022, 63, 34.		9
64	Objective Measures of Pre-lens Tear Film Dynamics versus Visual Responses. Optometry and Vision Science, 2016, 93, 872-880.	0.6	8
65	The intrinsically photosensitive retinal ganglion cell (ipRGC) mediated pupil response in young adult humans with refractive errors. Journal of Optometry, 2022, 15, 112-121.	0.7	8
66	Changes in Retinal Optical Coherence Tomography Angiography Indexes Over 24 Hours. , 2022, 63, 25.		8
67	Use of focus measure operators for characterization of flood illumination adaptive optics ophthalmoscopy image quality. Biomedical Optics Express, 2018, 9, 679.	1.5	7
68	Choroidal Thickness in Indigenous Australian Children. Translational Vision Science and Technology, 2020, 9, 28.	1.1	7
69	Custom extraction of macular ganglion cell-inner plexiform layer thickness more precisely co-localizes structural measurements with visual fields test grids. Scientific Reports, 2020, 10, 18527.	1.6	7
70	Automatic Retinal and Choroidal Boundary Segmentation in OCT Images Using Patch-Based Supervised Machine Learning Methods. Lecture Notes in Computer Science, 2019, , 215-228.	1.0	7
71	OCT Retinal and Choroidal Layer Instance Segmentation Using Mask R-CNN. Sensors, 2022, 22, 2016.	2.1	7
72	Anterior segment optical coherence tomography (AS-OCT) image analysis methods and applications: A systematic review. Computers in Biology and Medicine, 2022, 146, 105471.	3.9	7

DAVID ALONSO-CANEIRO

#	Article	IF	CITATIONS
73	Constructing Synthetic Chorio-Retinal Patches using Generative Adversarial Networks. , 2019, , .		6
74	Associations between seven-year C-reactive protein trajectory or pack-years smoked with choroidal or retinal thicknesses in young adults. Scientific Reports, 2021, 11, 6147.	1.6	6
75	Detection of clustered anomalies in single-voxel morphometry as a rapid automated method for identifying intracranial aneurysms. Computerized Medical Imaging and Graphics, 2021, 89, 101888.	3.5	6
76	Deep learning approaches for segmenting Bruch's membrane opening from OCT volumes. OSA Continuum, 2020, 3, 3351.	1.8	6
77	Clinical Evaluations of Macular Structure-Function Concordance With and Without Drasdo Displacement. Translational Vision Science and Technology, 2022, 11, 18.	1.1	6
78	The effect of transverse ocular magnification adjustment on macular thickness profile in different refractive errors in community-based adults. PLoS ONE, 2022, 17, e0266909.	1.1	6
79	Prediction of Retinal Ganglion Cell Counts Considering Various Displacement Methods From OCT-Derived Ganglion Cell–Inner Plexiform Layer Thickness. Translational Vision Science and Technology, 2022, 11, 13.	1.1	6
80	Segmentation of anterior segment boundaries in swept source OCT images. Biocybernetics and Biomedical Engineering, 2021, 41, 903-915.	3.3	5
81	Anterior scleral thickness and shape changes with different levels of simulated convergence. Experimental Eye Research, 2021, 203, 108435.	1.2	4
82	Static compression optical coherence elastography to measure the mechanical properties of soft contact lenses. Biomedical Optics Express, 2021, 12, 1821.	1.5	4
83	Evaluation of focus and deep learning methods for automated image grading and factors influencing image quality in adaptive optics ophthalmoscopy. Scientific Reports, 2021, 11, 16641.	1.6	4
84	Application of Deep Learning Methods for Binarization of the Choroid in Optical Coherence Tomography Images. Translational Vision Science and Technology, 2022, 11, 23.	1.1	4
85	OCT chorio-retinal segmentation with adversarial loss. , 2021, , .		4
86	Prediction of visual field defects from macular optical coherence tomography in glaucoma using cluster analysis. Ophthalmic and Physiological Optics, 2022, 42, 948-964.	1.0	4
87	Computationally efficient interference detection in videokeratoscopy images. , 2008, , .		3
88	Ganglion cell-inner plexiform layer measurements derived from widefield compared to montaged 9-field optical coherence tomography. Australasian journal of optometry, The, 2022, 105, 822-830.	0.6	3
89	OCT retinal image-to-image translation: Analysing the use of CycleGAN to improve retinal boundary semantic segmentation. , 2021, , .		3
90	Context-based modelling of interferometric signals for the assessment of tear-film surface quality. , 2009, , .		2

DAVID ALONSO-CANEIRO

#	Article	IF	CITATIONS
91	Swept source OCT with air puff chamber for corneal dynamics measurements. Proceedings of SPIE, 2012, , .	0.8	2
92	Comparison of Subjective and Objective Methods of Corneoscleral Limbus Identification from Anterior Segment Optical Coherence Tomography Images. Optometry and Vision Science, 2021, 98, 127-136.	0.6	2
93	Retinal Differential Light Sensitivity Variation Across the Macula in Healthy Subjects: Importance of Cone Separation and Loci Eccentricity. Translational Vision Science and Technology, 2021, 10, 16.	1.1	2
94	Non-invasive assessment of corneal crosslinking changes using polarization sensitive optical coherence tomography. Proceedings of SPIE, 2013, , .	0.8	1
95	Precise geometry of the anterior chamber of the eye by means of OCT imaging Photonics Letters of Poland, 2018, 10, 67.	0.2	1
96	Quantitative compressive optical coherence elastography using structural OCT imaging and optical palpation to measure soft contact lens mechanical properties. Biomedical Optics Express, 2021, 12, 7315.	1.5	1
97	Dual image and mask synthesis with GANs for semantic segmentation in optical coherence tomography. , 2020, , .		1
98	Use of uncertainty quantification as a surrogate for layer segmentation error in Stargardt disease retinal OCT images. , 2021, , .		1
99	The effect of intrinsically photosensitive retinal ganglion cell (ipRGC) stimulation on axial length changes to imposed optical defocus in young adults. Journal of Optometry, 2022, , .	0.7	Ο